ELSEVIER

Journal of Photochemistry and Photobiology A: Chemistry 134 (2000) 59–70

Journal of Photochemistry and Photobiology A:Chemistry

www.elsevier.nl/locate/jphotochem

Quantum yields and relative photonic efficiencies of substituted 1,3-dihydroxybenzenes

Ayse Neren Ökte, Marianne Sowa Resat[1], Yüksel Inel*

Department of Chemistry, Bogazici University, P.K. 2 Bebek, 80815 Istanbul, Turkey

Received 14 February 2000; accepted 21 February 2000

Abstract

1,3-dihyroxybenzene (1,3-DHB) is selected as the standard probe and Degussa P25 TiO_2 as the standard photocatalyst for the determination of quantum yields of 3,5-dihydroxytoluene (3,5-DHT), 1,3-dihydroxy-5-methoxybenzene (1,3-DHMB), and 3,5-dihydroxybenzoic acid (3,5-DHBA) based on the relative photonic efficiency concept. A detailed analysis about the incident photon flux and rate of formation of CO_2 for the photocatalytic degradation of 1,3-DHB is done. Fraction of light absorption is measured as a function of incident photon flux and TiO_2 loading. When a TiO_2 concentration of 1 g/l and an incident photon flux of 10.8×10^{-6} Einstein/min are used, the quantum yields for the photocatalytic degradation of 1,3-DHB, based on disappearance of 1,3-DHB, and formation of CO_2 are found as 0.06 and 0.34, respectively. The difference between two quantum yields indicate the formation of intermediates during the photodegradation process. The effect of reactant concentration, pH of the medium and temperature of the system are investigated to determine the relative efficiencies of the reactant molecules. Quantum yields of the reactants are found from $\phi=\zeta_r\,\phi_{1,3\text{-DHB}}$ at their natural pH values as 0.22, 0.35, and 0.38 for 3,5-DHT, 1,3-DHMB and 3,5-DHBA, respectively.

Keywords: Titanium dioxide; 1,3-Dihydroxybenzene; Substituted 1,3-dihydroxybenzenes; Relative photonic efficiency; Quantum yield

1. Introduction

Heterogeneous photocatalysis being an emerging technology has been extensively studied over the past two decades by utilizing illuminated semiconductors. Recent reviews about the photocatalysis are provided by Ollis and Al-Ekabi [1], Fox and Dulay [2], Legrini et al. [3], Hoffmann et al. [4], and Mills and Hunte [5].

When factors concerning photostability, toxicity, cost, availability, and redox efficiencies are all considered TiO_2 has turned out to be the photocatalyst of choice. TiO_2 is active for light reduced redox processes due to its electronic structure, which is characterized by a filled valence band and an empty conduction band. When a photon with an energy of $h\nu$ exceeds the bandgap energy, E_{bg}, of TiO_2 (3.2 eV), an electron is promoted from the valence band into the conduction band, leaving a hole behind. Excited state conduction band electrons and valence band holes can recombine and dissipate the input energy as heat, get trapped in surface states, or react with electron donors and electron acceptors adsorbed on TiO_2 surface or within the surrounding layer of the charged particles.

Photocatalytic efficiency is controlled by the effectiveness of suppression of electron–hole recombination. This is also affected by reaction conditions, such as pH of the medium, concentration of the substrate molecule, temperature of the photocatalytic system, and incident photon absorption. What has been lacking is the measurement of the apparent quantum yield. It has proved that the measurement of quantum yield in heterogeneous photocatalytic processes is very difficult because of the problem of light scattering [6].

Quantum yield (ϕ) expresses the number of molecules, N_{mol}, undergoing a reaction relative to the number of quanta, N_{photon}, absorbed by the photocatalyst (Eq. (1)).

$$\phi=\frac{N_{mol}\ (\text{mol/s})}{N_{photon}\ (\text{Einstein/s})}=\frac{\text{rate of reaction}}{\text{rate of absorption of photons}} \quad (1)$$

The reason is that the rate of absorption of photons is very difficult to assess, since semiconductor particles will absorb, scatter, and transmit light. TiO_2 particulates are not capable

* Corresponding author. Tel.: +90-212-263-1540/1610 or 1619; fax: +90-212-287-2467.

E-mail addresses: marianne.sowa-resat@pnl.gov (M.S. Resat), yinel@boun.edu.tr (Y. Inel)

[1] Present address: Pacific Northwest National Lab, PO Box 999, MS K8-88, Richland, WA 99352, USA.

1010-6030/00/$ – see front matter
PII: S1010-6030(00)00246-X

of absorbing all the incident photon flux from a given source due to the light scattering off the particle surface. The intensity of light scattered by the suspension depends on the refractive indices of the scattering molecule/particle (n_1) and the surrounding medium (n_0) [5]. For the materials making up a typical photocatalytic system in heterogeneous photocatalysis, n_0 is 1.33 for H_2O and n_1 is 1.5–1.7 for glass, 3.87 for rutile TiO_2, and ~2.5–3 for anatase TiO_2 all at 365 nm [7]. When $n_0 \approx n_1$, the extent of scattered light is negligible. When $n_1 > n_0$, light is expected to be highly scattered, with losses of ~5–10% of the light flux occurring. The percentage of photons absorbable appear to be in the range of ~50–65% [7].

In defining Eq. (1), properties of the catalyst surface are important since the course of reactions depends on the characteristics of the surface upon light activation. Also, light activated steps play major roles in defining the quantum yield. These steps include photon absorption, the formation of the hydroxyl radicals on the catalyst surface, and catalytic steps including adsorption/desorption events and reaction of the hydroxyl radicals with the adsorbed substrate [8]. However, all the surface sites occupied by OH^- groups are not catalytically active. Also, depending on the reactor geometry, particle aggregation, and stirring, not all of the BET catalyst surface is accessible to the substrate being oxidized.

A more useful term, photonic efficiency, ζ, has been proposed by Serpone et al. [9] to compare process efficiencies and to avoid the confusion with quantum yields reported in the literature. Photonic efficiency (ζ) describes the number of reactant molecules transformed or product molecules formed divided by the number of photons at a given wavelength.

$$\zeta = \frac{N_{\text{molecules}}\ (\text{mol/s})\ \text{produced}}{N_{\text{photons}}\ (\text{Einstein/s})\ \text{incident inside reactor cell}} \quad (2)$$

The relative photonic efficiency, ζ_r, is related to a standard photocatalyst and a standard secondary actinometer in photocatalyzed processes. Extensive studies have confirmed the usefulness of ζ_r [9]. The initial photodegradation of phenol was chosen as the standard process and Degussa P25 TiO_2 as the standard photocatalyst, and ζ_r is defined as

$$\zeta_r = \frac{\text{rate of disappearance of substrate}}{\text{rate of disappearance of phenol}} \quad (3)$$

where both initial rates are obtained under exactly the same conditions. Ultimately, ζ_r can be converted into the quantum yield, ϕ, once a quantum yield, ϕ_{standard}, for a given photocatalyst and a given substrate has been determined (Eq. (4)).

$$\phi = \zeta_r \phi_{\text{standard}} \quad (4)$$

The present report is an application of relative photonic efficiency concept for three phenolic substrates: 3,5-dihydroxytoluene (3,5-DHT), 1,3-dihydroxy-5-methoxybenzene (1,3-DHMB), and 3,5-dihydroxybenzoic acid (3,5-DHBA). To determine the quantum yields of all reactant molecules, 1,3-dihyroxybenzene (1,3-DHB) is selected as the standard probe and Degussa P25 TiO_2 as the standard photocatalyst. Thus, a detailed analysis about the incident photon flux and rate of formation of CO_2 for the photocatalytic degradation of 1,3-DHB is performed. The effects of pH, concentration of reactant and temperature on ζ_r are examined for the photodegradation of three substituted 1,3-DHBs: 3,5-DHT, 1,3-DHMB and 3,5-DHBA.

2. Experimental

2.1. Reagents

Degussa P25 grade titanium dioxide was used as the photocatalyst. The average particle size was 30 nm. The BET surface area was $50 \pm 15\ m^2/g$. X-ray diffraction data has confirmed that the TiO_2 is predominantly in the anatase form.

3,5-DHBA was Aldrich, 1,3-DHB, 3,5-DHT and 1,3-DHMB were Fluka chemicals used in the experiments without further purification. Singly distilled water was deionized and used for the preparation of all solution.

2.2. The gas recycling reactor

All photodegradation experiments were performed in a gas recycling reactor, details of which have been published previously [10]. Briefly, the reactor consists of a 36.2 cm long Pyrex tube with an inner diameter of 3.5 cm. To allow temperature regulation via water circulation, there is a sealed inner glass tube in the gas recycling reactor with a thickness of 2 cm. The TiO_2 suspension is contained in the annulus formed between the two tubes. The gas above the suspension is pumped using a Cole–Palmer peristaltic pump. A sintered glass disk, placed at the bottom of the reactor, provides circulation of air and prevents settlement of the suspension. All connections were made with Tygon tubing.

The reactor is located in an irradiation box (70 cm × 22 cm) containing six 20 W black light fluorescent lamps (General Electric F 20 T 12/BLB) that provide light of wavelength 320–440 nm. The lamps are positioned to surround the reaction vessel from three sides. Lamps can be lit individually as well as in conjunction with each other. The front side of the irradiation box was designed to operate as a door with the reactor attached. This maintains a uniform geometry throughout the experiments. A fan was placed at the top of the box and air was also continually circulated through the box in order to eliminate any heating effects of the lamps.

2.3. Sample preparation

Stock solutions of reactant molecules are prepared as 100 μM at their natural pH conditions, a catalyst concentration of 1 g/l of TiO_2, and a 144 ml/min of flow rate of

air were used for all experiments unless otherwise stated [10]. Prior to the photodegradation experiments, the suspension (containing 200 ml of the substrate and 1 g/l of TiO_2) was stirred for 30 min in the dark to achieve an adsorption equilibrium for the substrate on the photocatalyst. Solutions were always kept in the dark in order to prevent any interference from ambient light prior to irradiation. The pH values of the reaction solutions were adjusted by adding NaOH or $HClO_4$.

2.4. Analysis

The amount of CO_2 produced during reactions was determined by a Shimadzu (Gow Mac) gas chromatograph equipped with a thermal conductivity detector and a Porapak N column. Helium was used as a carrier gas at a flow rate of 60 ml/min. Calibrations were carried out using measured volumes of CO_2 added to the gas phase loop under identical conditions with the experiments. Sampling was made from the top of the reactor on which a mini inert valve is attached.

Following photodegradation, the concentration of substrate remaining was analyzed by high performance liquid chromatograph (HPLC, CECIL 1100 series), using a CE 1100 liquid chromatography pump with CE 1220 variable wavelength monitor and a UV-detector. The stationary phase was a Hypersil ODS column (particle size 10 μm). The mobile phase was a methanol:water (50:50) mixture. The measurements were performed at λ=274 nm. All samples were filtered using Millipore films (0.45 μm) before injection.

Table 1
Effect of incident photon flux (I_0) in 30 min irradiation time

Number lamps	$I_0 \times 10^{-6}$ (Einstein/min)	[1,3-DHB][a] (μM)	[CO_2][b] (μM)
–	–	100	0
1	1.8	88.7	3.25
2	3.6	81.6	11.7
3	5.4	69.9	21.3
4	7.2	62.4	31.5
5	9.0	54.9	39.7
6	10.8	17.4	40.3

[a] [1,3-DHB]: each numerical value represents the percent of 1,3-DHB remaining in the solution.
[b] [CO_2]: each numerical value represents the percent of CO_2 formation.

3. Results and discussion

3.1. Effect of incident photon flux on the degradation of 1,3-DHB

The incident photon flux for each lamp is measured using potassium ferrioxalate actinometry. It is found that each lamp emits 1.8×10^{-6} Einstein/min in the wavelength region (300–400 nm).

When the percent concentration of 1,3-DHB remaining in solution and the percent of CO_2 formation are plotted together for 30 min irradiation time for various incident photon fluxes, the maximum amount of CO_2 formation and the minimum amount of 1,3-DHB concentration in solution, i.e. maximum degradation of 1,3-DHB, are obtained with six lamps (10.8×10^{-6} Einstein/min) (Fig. 1, Table 1).

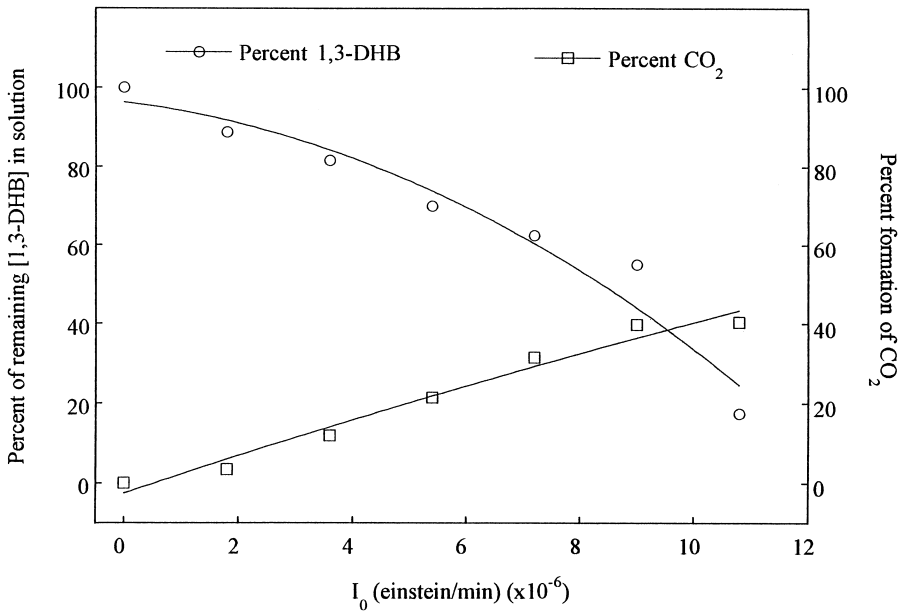

Fig. 1. The percent of 1,3-DHB remaining in solution and the percent of CO_2 formation as a function of incident photon flux. Conditions: [TiO_2]=1 g/l, flow rate=144 ml/min, [1,3-DHB]$_0$=100 μM, pH=5.4, T=298 K.

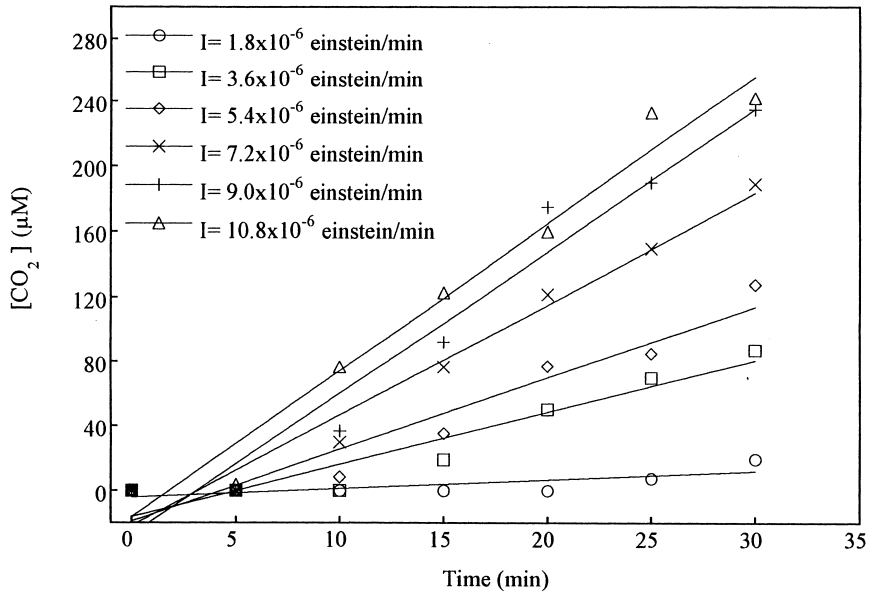

Fig. 2. Effect of incident photon flux on the concentration of CO_2 produced. Conditions: $[TiO_2]$=1 g/l, flow rate=144 ml/min, $[1,3\text{-DHB}]_0$=100 μM, pH=5.4, T=298 K.

Fig. 2 shows the relation between formation of CO_2 and the incident photon flux, I_0. It indicates that increasing the number of lamps increases the amount of CO_2 formation from a 100 μM 1,3-DHB solution. This is because increasing the incident photon flux increases the production rate of electron–hole pairs. However, the opportunity for electron–hole recombination also increases. Thus, the relative number of the photoinduced carriers taking part in the redox reactions on the surface of TiO_2 decreases. This results in a decrease of formation rate of CO_2 when the flux is high (Fig. 3, Table 2). When rate is plotted versus the square root of incident photon flux, a better linearity is obtained, which indicates the validity of the above discussion (Fig. 3 inset).

3.2. Determination of quantum yield

TiO_2 particles are not capable of absorbing all the incident photon flux from a given source due to the light scattering off the particle surface. Sun and Bolton [6] used an integrated

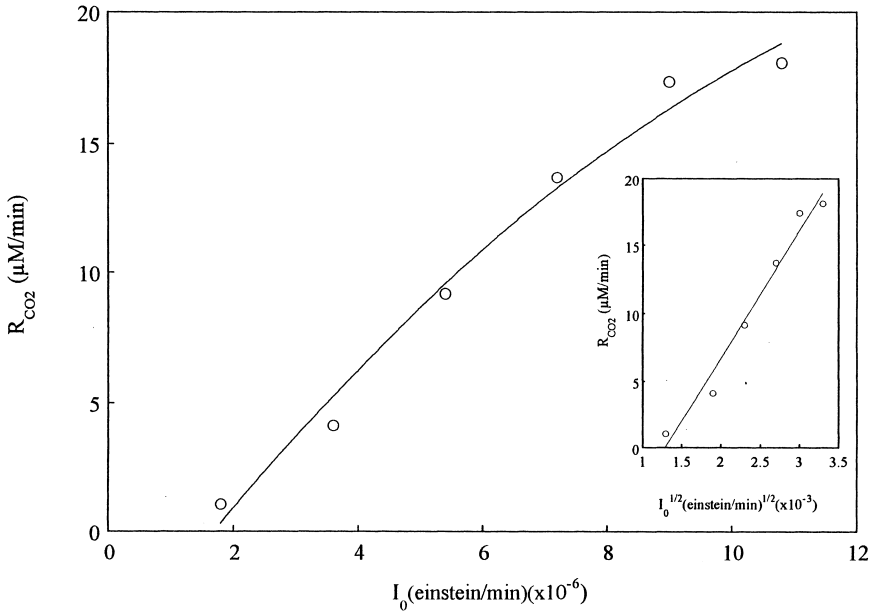

Fig. 3. Rate of CO_2 production vs. incident photon flux. Inset: R_{CO_2} as a function of $1/(I_0)^{1/2}$. Conditions: $[TiO_2]$=1 g/l, flow rate=144 ml/min, $[1,3\text{-DHB}]_0$=100 μM, pH=5.4, T=298 K.

Table 2
Effect of incident photon flux on the rate of CO_2 formation

$I_0\times10^{-6}$ (Einstein/min)	$(I_0)^{1/2}\times10^{-3}$ (Einstein/min)$^{1/2}$	$R_{CO_2}\times10^{-7}$ (mol/min)
1.8	1.3	1.06
3.6	1.9	4.11
5.4	2.3	9.18
7.2	2.7	13.7
9.0	3.0	17.4
10.8	3.3	18.1

Table 3
Fraction of light absorption '*f*' and quantum yield 'ϕ' as a function of incident photon flux in the presence of 1 g/l TiO_2

TiO_2 loading (g/l)	$I_0\times10^{-6}$ (Einstein/min)	*f*	ϕ
1.00	3.058[a]	0.1385[a]	0.14[a]
1.00	3.600	0.163[b]	0.21[b]

[a] Values are from Serpone's paper for degradation of phenol [8].
[b] Calculated fraction of absorption and quantum yield for degradation of 1,3-DHB.

sphere to estimate the fraction of light absorbed in a TiO_2 suspension. The principle of the integrated sphere model is that, when incident light of flux I_0 passes through a sample, light both from that transmitted through the sample and that scattered from the particles, can be completely reflected by an inner highly reflecting surface. The light radiation level in the sphere can then be monitored by a detector.

Serpone [8] used the integrating sphere method to determine the fraction of light absorbed by Degussa P25 TiO_2. It is found that there is a significant deviation between the absorbance spectra of the 100 mg/l titania sample using the integrating sphere method and the spectrum of the titania sample obtained using normal spectroscopic methods. The fraction of light absorbed is found by the difference between the response of the instrument for a solution with no titania particles and the response of the instrument for the titania colloidal. In the study, phenol was used as the standard process and the quantum yield, ϕ ($\phi=\zeta_r\,\phi_{Phenol}$) was determined from relative photonic efficiency, ζ_r, and the quantum yield for the photocatalyzed degradation of phenol (ϕ_{Phenol}).

Since 1,3-DHB is the standard probe in our study, we need to know the apparent quantum yield for 1,3-DHB ($\phi_{1,3\text{-DHB}}$) to convert the relative photonic efficiencies into the corresponding quantum yields of photodegradation of 3,5-DHT, 1,3-DHMB and 3,5-DHBA ($\phi=\zeta_r\,\phi_{1,3\text{-DHB}}$). We follow Serpone's results to find the quantum yield for the photocatalyzed oxidative degradation of 1,3-DHB [8].

Serpone changed the TiO_2 loading from 0.1 to 4 g/l and estimated the fraction of light absorbed assuming Beer's law to be followed at higher TiO_2 loadings. For 1 g/l TiO_2 loading and 3.058×10^{-6} Einstein/min incident photon flux, the fraction of the absorption value was found as 0.1385.

The following assumptions are used in our study:

1. We have monitored the formation of CO_2 varying the incident photon flux in the presence of 1 g/l TiO_2 (Fig. 2). The second studied flux, with a value of 3.6×10^{-6} Einstein/min, is close to the value 3.058×10^{-6} Einstein/min with 1 g/l TiO_2 loading and a value of 0.1385 fraction of absorption in Serpone's paper. In order to find the fraction of light absorption with 3.6×10^{-6} Einstein/min incident intensity, we multiply the value 0.1385, with a factor of 1.18 (assuming linearity between the incident photon flux and the fraction of light absorption), which comes from the ratio between 3.6×10^{-6} and 3.058×10^{-6} Einstein/min. As a result, the fraction of absorption for 3.6×10^{-6} Einstein/min is found as 0.163 (Table 3).
2. Since absorption varies linearly with the incident photon flux, according to Beer's law, we assume the same linearity between the fraction of light absorption and the incident photon flux. Thus, for the studied incident intensities, the corresponding fractions of absorptions and the quantum yields for the formation of CO_2 and for the degradation of 1,3-DHB in 30 min irradiation time are calculated (Table 4).

   The initial rates of formation of CO_2 and degradation of 1,3-DHB show deviations from linearity as the incident intensity increases (Fig. 4 and inset). This is an expected result since increasing the photon flux increases the opportunity for electron–hole recombination. An analogous trend is observed when quantum yields are evaluated with respect to incident photon flux (Fig. 5 and inset).
3. The amount of TiO_2 loading is also investigated for the production of CO_2 by using a constant incident photon flux, 10.8×10^{-6} Einstein/min. Serpone estimated

Table 4
Quantum yields as a function of incident photon flux[a,b]

$I_0\times10^{-6}$ (Einstein/min)	*f*	$R_{CO_2}\times10^{-7}$ (mol/min)	$R_{1,3\text{-DHB}}\times10^{-7}$ (mol/min)	ϕ_{CO_2}	$\phi_{1,3\text{-DHB}}$
1.8	0.082	1.06	0.75	0.72	0.51
3.6	0.163	4.11	1.23	0.70	0.21
5.4	0.245	9.18	2.01	0.69	0.15
7.2	0.326	13.7	2.51	0.58	0.11
9.0	0.408	17.4	3.01	0.47	0.08
10.8	0.489	18.1	3.11	0.34	0.06

[a] R_{CO_2}: rate of formation of CO_2. $R_{1,3\text{-DHB}}$: rate of degradation of 1,3-DHB.
[b] Condition: $[TiO_2]=1.00$ g/l.

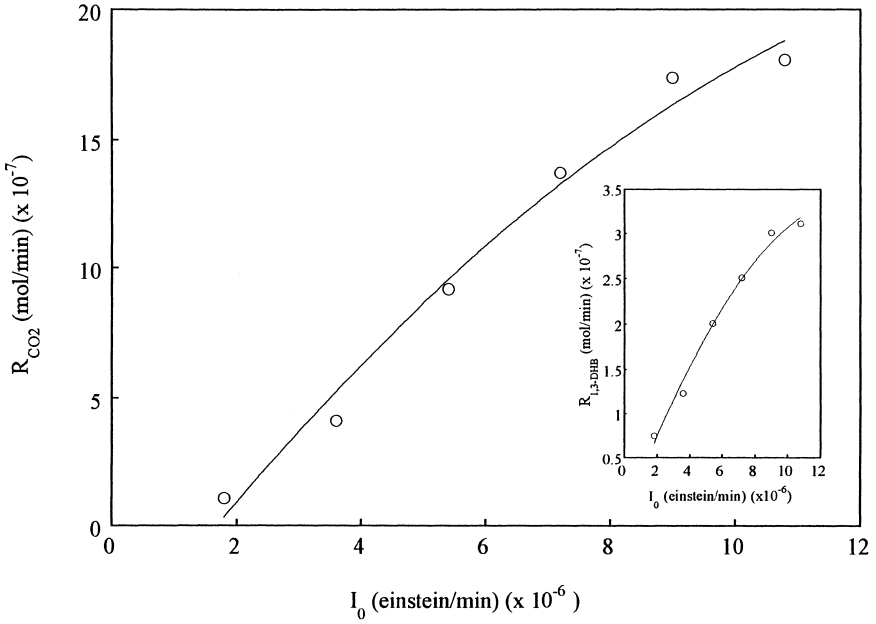

Fig. 4. Rate of CO_2 production vs. incident photon flux. Inset: $R_{1,3\text{-DHB}}$ as a function of I_0. Conditions: [TiO_2]=1 g/l, flow rate=144 ml/min, [1,3-DHB]$_0$=100 μM, pH=5.4, T=298 K.

the fraction of light absorbed at concentrations greater than 0.10 g/l TiO_2 loadings by using Beer's law. We made the same estimation for the concentrations greater and lower than 1.00 g/l TiO_2, i.e. a linear increase is assumed for concentrations greater than 1.00 g/l, and a linear decrease is assumed for concentrations lower than 1.00 g/l. Quantum yields are calculated according to the estimated fractions of absorption (Table 5).

Fig. 6 shows that the initial rate of CO_2 production and the initial rate of 1,3-DHB degradation increase linearly from 0.10 to 1.00 g/l loading and then exhibits a negative deviation at 4 g/l. Since, as the titania loading increases, the suspension becomes more opaque to light, only photons absorbed by titania particles onto which a 1,3-DHB molecule is pre-adsorbed may be effective in carrying out the redox chemistry. Dependence of quantum yields on the loading of

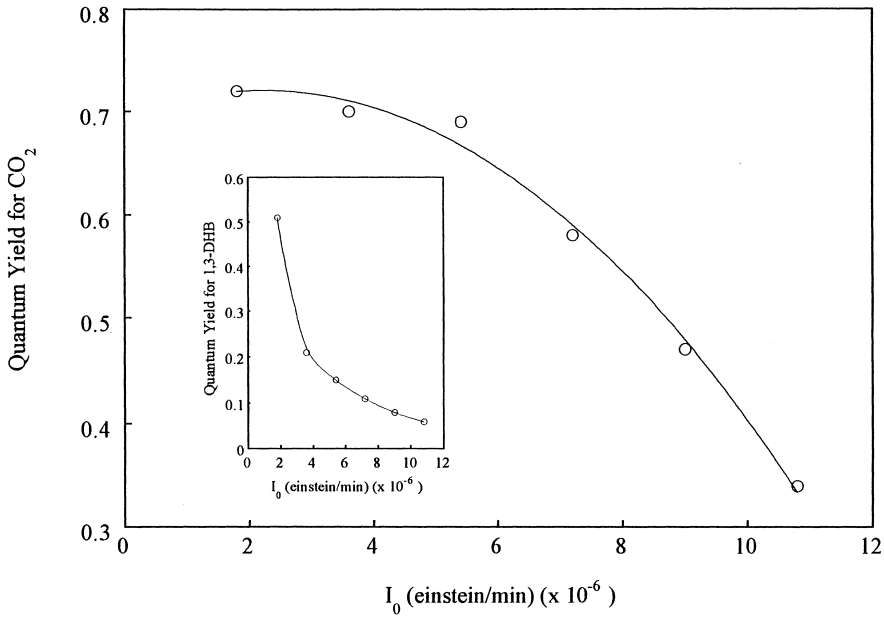

Fig. 5. Quantum yield for CO_2 production as a function of incident photon flux. Inset: quantum yield for 1,3-DHB degradation as a function of I_0. Conditions: [TiO_2]=1 g/l, flow rate=144 ml/min, [1,3-DHB]$_0$=100 μM, pH=5.4, T=298 K.

Table 5
Quantum yields as a function of TiO_2 loadings[a]

TiO_2 loading (g/l)	f	$R_{CO_2}\times10^{-7}$ (mol/min)	$R_{1,3\text{-DHB}}\times10^{-7}$ (mol/min)	ϕ_{CO_2}	$\phi_{1,3\text{-DHB}}$
0.10	0.049	7.93	1.32	1.51	0.25
0.30	0.147	9.81	1.63	0.62	0.10
0.50	0.245	12.8	2.13	0.48	0.08
1.00	0.489	18.1	3.02	0.34	0.06
2.00	0.978	15.3	2.55	0.14	0.02
4.00	1.956	7.93	1.32	0.04	0.006

[a] Condition: $I_0=10.8\times10^{-6}$ Einstein/min.

TiO_2 are given in Fig. 7. The decreasing trends in quantum yields as a function of TiO_2 loading are expected. However, the quantum yield for CO_2 formation in 0.10 g/l TiO_2 loading exceeds the maximum theoretical value of 1.00. This suggests there is some error introduced in our use of Serpone's results to estimate quantum yields under different experimental conditions. A possible cause for this are the differences between the fractions of light absorption for phenol degradation and the fractions of light absorption for the formation of CO_2 in 1,3-DHB degradation. When these two fractions are plotted together (Fig. 8), the ratio between the slopes is found as 4.40. If we correct the quantum yield of 1.51 according to slope ratio 4.40, we can obtain the quantum yield for 0.10 g/l TiO_2 loading as 0.34. Since we are looking for relative photonic efficiencies, and all data exhibit the expected increase according to Beer's law, this should not affect relative values.

Since throughout our study a TiO_2 concentration of 1 g/l and the incident photon flux of 10.8×10^{-6} Einstein/min are used, the relative photonic efficiencies of the compounds 3,5-DHT, 1,3-DHMB and 3,5-DHBA will be converted into the corresponding quantum yields using $\phi=\zeta_r\phi_{1,3\text{-DHB}}$ where $\phi_{1,3\text{-DHB}}=0.06$, or $\phi=\zeta_r\phi_{CO_2}$ where $\phi_{CO_2}=0.34$.

3.3. Photodegradation reactions

3.3.1. Effect of initial concentration of substrate

Fig. 9 displays the rate of CO_2 formation as a function of initial substrate concentration for all reactant molecules. For 1,3-DHB and 3,5-DHT, CO_2 formation is examined at four initial concentrations (10, 50, 100, 1000 μM), for 1,3-DHMB; at five initial concentrations (2000, 1000, 700, 500, and 100 μM) and for 3,5-DHBA; at four initial concentrations (1000, 200, 100 and 75 μM). Each of the substrate shows a sharp increase for lower concentrations, then a plateau is achieved for higher concentrations.

3.3.2. Effect of pH

The photocatalytic degradation of 1,3-DHB and substituted 1,3-DHBs are strongly dependent on the pH value of the corresponding substrate solutions. This dominant effect

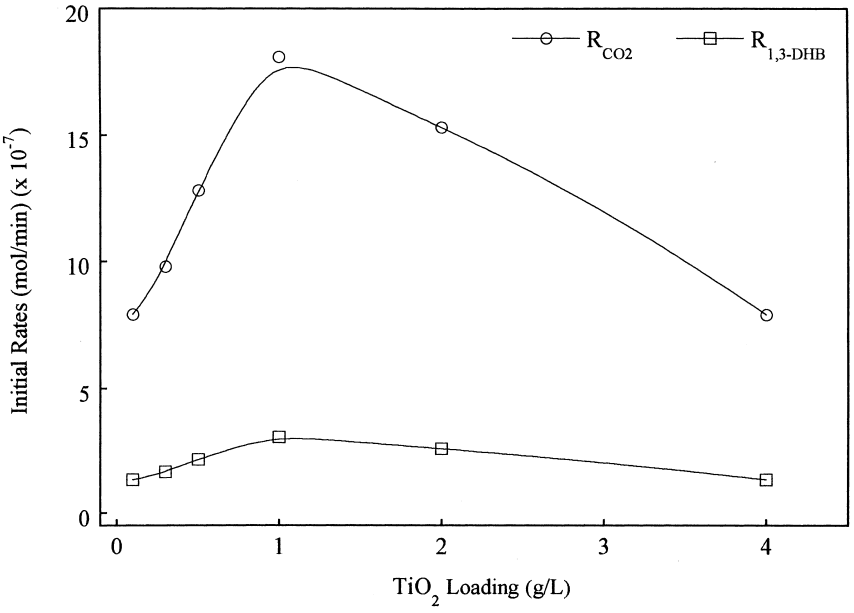

Fig. 6. Initial rate of CO_2 production and initial rate of 1,3-DHB degradation as a function of TiO_2 loading. Conditions: flow rate=144 ml/min, $[1,3\text{-DHB}]_0=100$ μM, pH=5.4, $T=298$ K, $I_0=10.8\times10^{-6}$ Einstein/min.

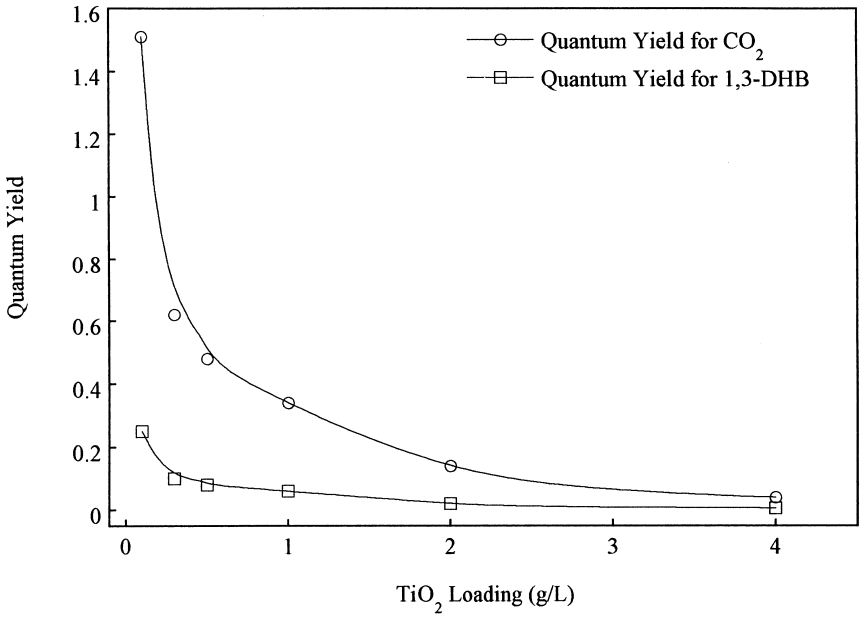

Fig. 7. Quantum yield for CO_2 production and quantum yield for 1,3-DHB degradation as a function of TiO_2 loading. Conditions: flow rate=144 ml/min, $[1,3\text{-DHB}]_0$=100 μM, pH=5.4, T=298 K, $I_0=10.8\times10^{-6}$ Einstein/min.

of pH is due to competitive factors including dissociation of reactant molecules (i.e. their pK values), adsorption of OH^- ions and adsorption of reactant ions on the surface of TiO_2.

The formation of CO_2 for the photocatalytic degradation of 1,3-DHB and substituted 1,3-DHBs are followed at different pH values; 3.5, 7.0, 9.0 and natural pH of the substrates. The highest rate is obtained at pH 9.0 for 1,3-DHB, 3,5-DHT, and 1,3-DHMB (Fig. 10A–C). For 3,5-DHBA, the highest rates are observed in acidic media. The lowest rate is obtained at pH 7.0, but increasing the solution pH to 9.0 increased the formation of CO_2 (Fig. 10D).

3.3.3. *Effect of temperature*

The effect of temperature on the rate of CO_2 formation is monitored in the range 298–333 K. For all temperatures

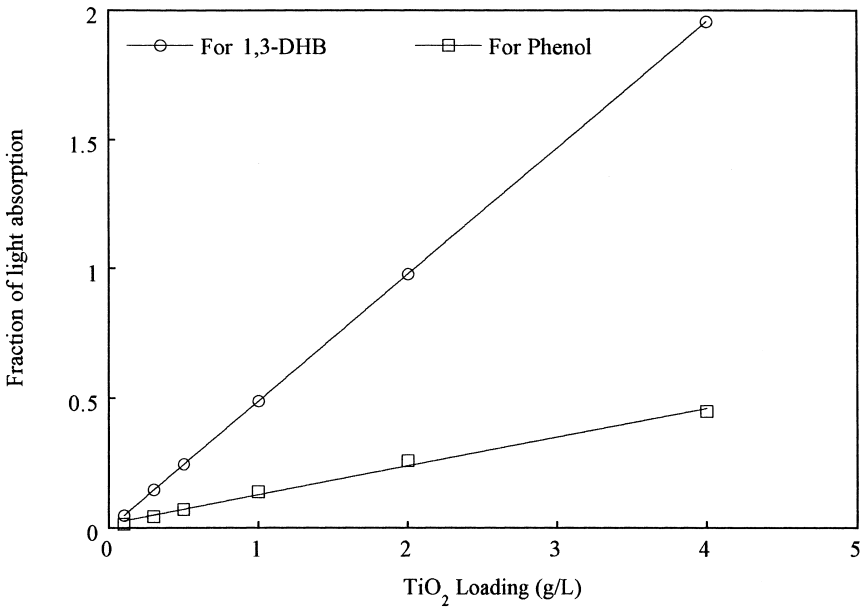

Fig. 8. Comparison between fraction of light absorption for phenol degradation and the fraction of light absorption for the formation of CO_2 in 1,3-DHB degradation.

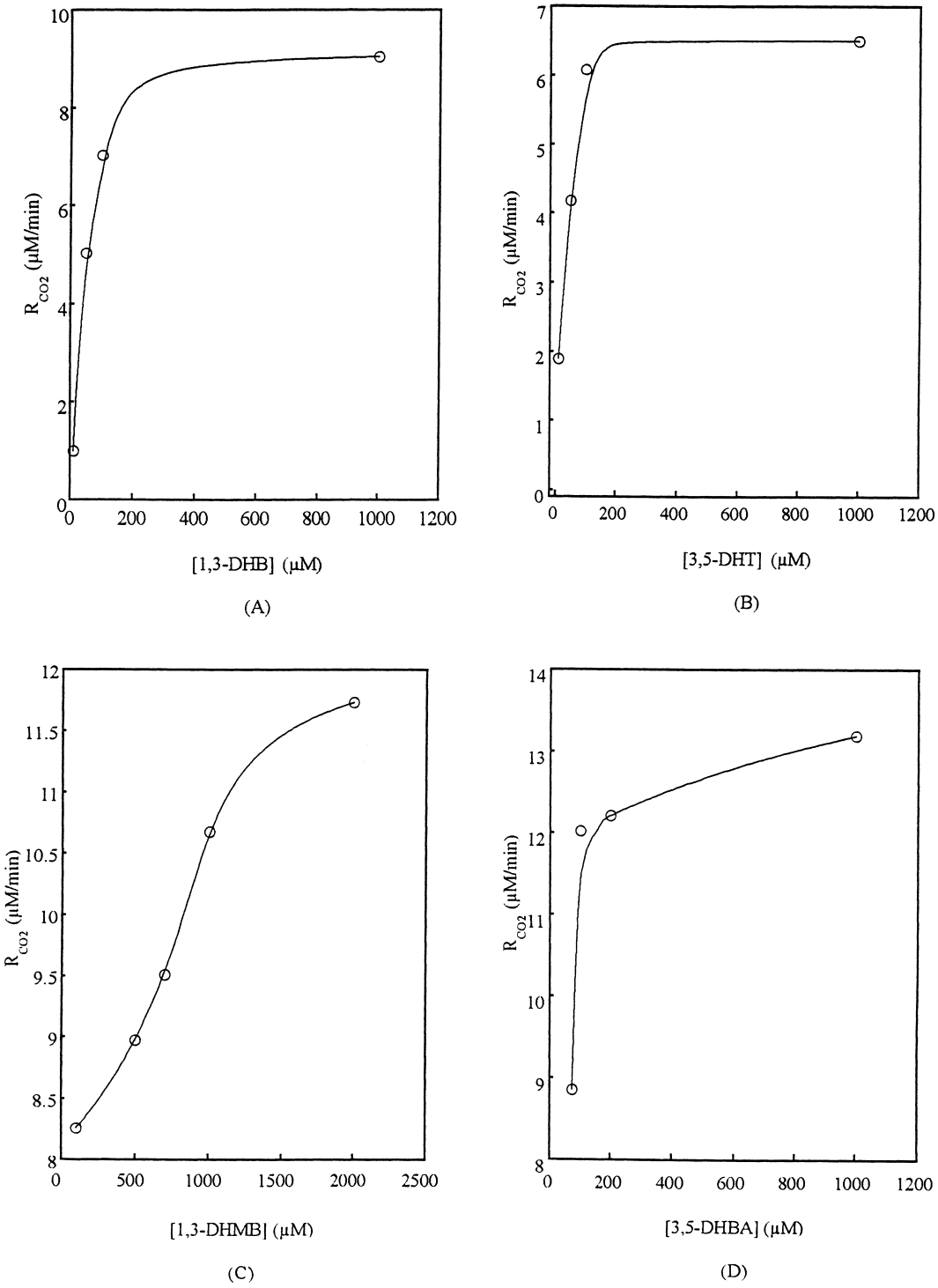

Fig. 9. Rate of CO_2 formation as function of reactant concentration: (A) for 1,3-DHB; (B) for 3,5-DHT; (C) for 1,3-DHMB and (D) for 3,5-DHBA.

studied, the rate is observed to increase for each substrate (Fig. 11).

3.4. Relative photonic efficiencies

The relative photonic efficiencies based on the rate of formation of CO_2 for 3,5-DHT, 1,3-DHMB and 3,5-DHBA are reported in Table 6. It is not possible to see a general trend for the relative photonic efficiencies as a function of the parameters changed. Some of the efficiencies are greater than unity indicating that the initial photocatalyzed oxidative degradation of selected substrates are more efficient than 1,3-DHB. However, some of the efficiencies are less than unity.

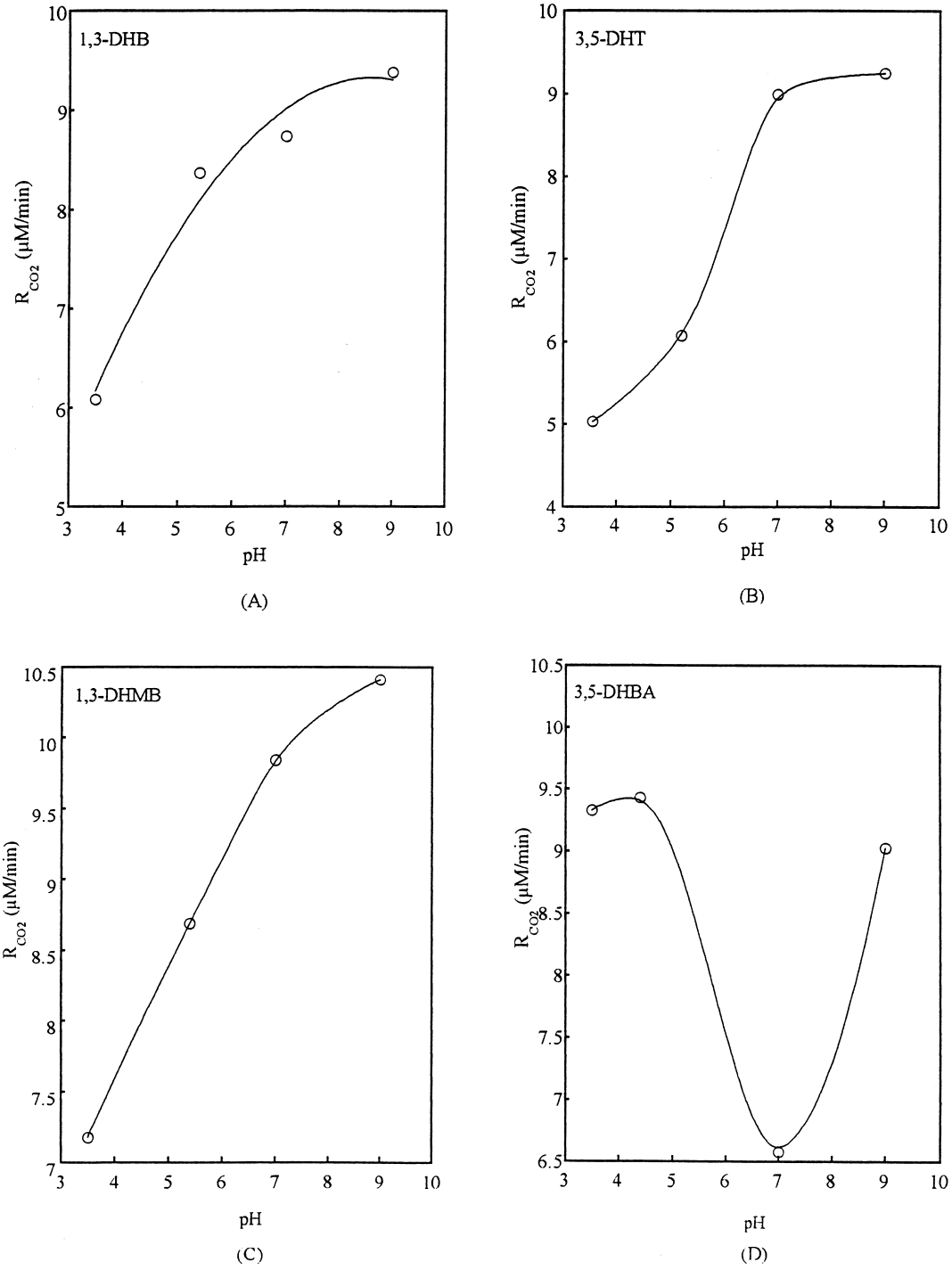

Fig. 10. Rate of CO_2 formation as function of pH: (A) for 1,3-DHB; (B) for 3,5-DHT; (C) for 1,3-DHMB and (D) for 3,5-DHBA.

According to substrate concentration, substrates containing electron donor groups ('CH_3' in the case of 3,5-DHT and 'OCH_3' in the case of 1,3-DHMB) show lower relative efficiencies compared to that containing an electron-withdrawing group ('COOH' in the case of 3,5-DHBA). However, with the increase in concentration, while relative photonic efficiencies of 1,3-DHMB and 3,5-DHBA increase, the efficiency of 3,5-DHT decreases. With respect to pH, for acidic media, relative efficiency is higher for 3,5-DHBA. This may be due to the lower p*K* value of 3,5-DHBA which results in higher degradation rates or percentages at low pH. By contrast, in alkaline media, 1,3-DHMB has the highest efficiency which corresponds to expected p*K* value of 9.81. In the neutral medium, 3,5-DHT and 1,3-DHMB have almost the same relative photonic efficiency whereas 3,5-DHBA has the lowest. When the

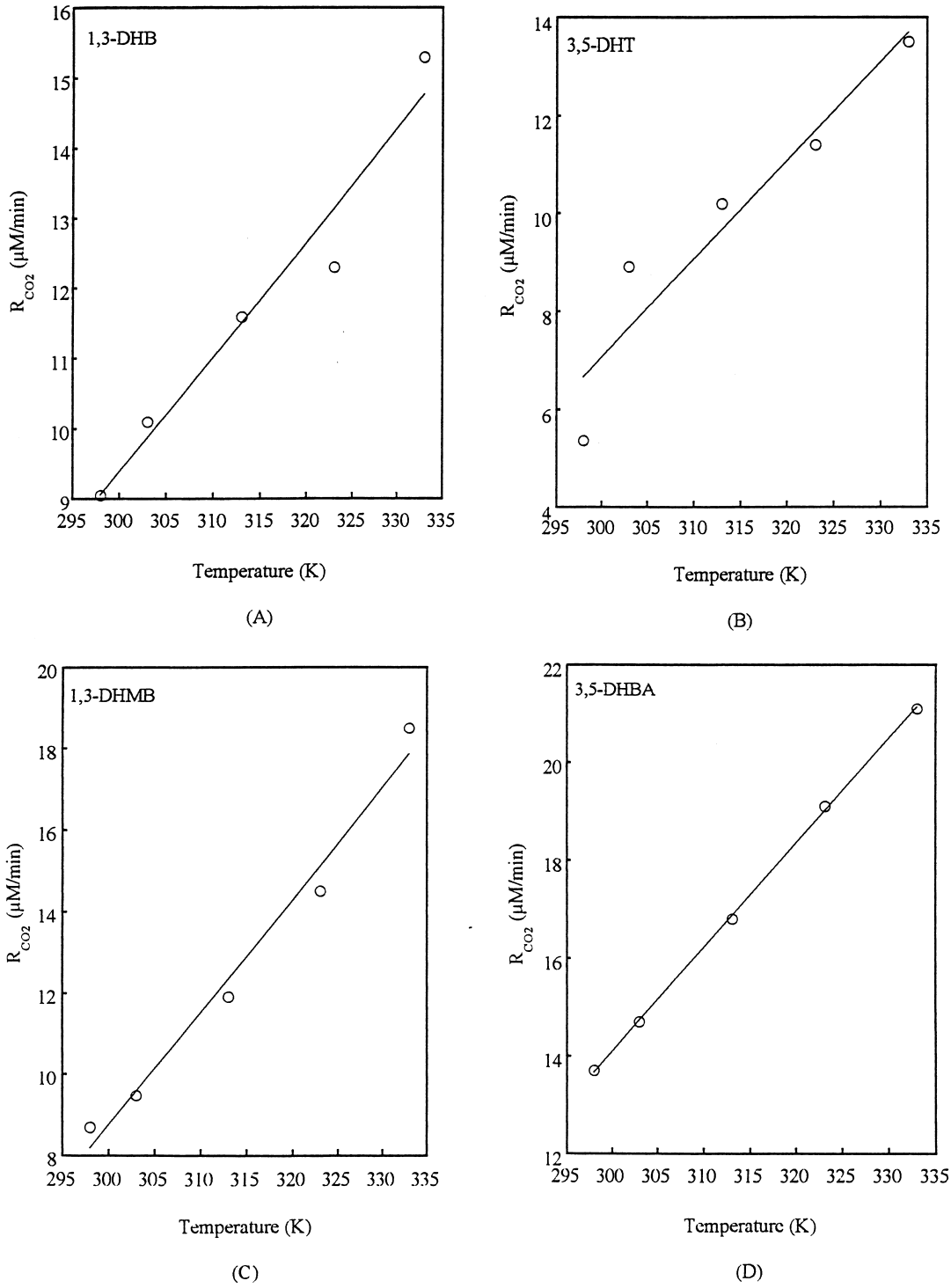

Fig. 11. Rate of CO_2 formation as function of temperature: (A) for 1,3-DHB; (B) for 3,5-DHT; (C) for 1,3-DHMB and (D) for 3,5-DHBA.

temperature is examined as a parameter, it is observed that increasing the temperature does not make a considerable change for the efficiencies. However, when electron donor substituents of 3,5-DHT and 1,3-DHMB are compared with the electron-withdrawing substituent of 3,5-DHBA, higher efficiencies are obtained with the latter.

We would expect that electron donor groups, CH_3 and OCH_3, in 3,5-DHT and 1,3-DHMB, respectively, increase the electron density over the aromatic ring and facilitate the attack by electrophilic $^{\bullet}OH$ radicals. Thus, the electron-withdrawing group, COOH in the presence of 3,5-DHBA is expected to decrease the electron density over

Table 6
Relative photonic efficiencies for 3,5-DHT, 1,3-DHMB and 3,5-DHBA under various conditions relative to 1,3-DHB

Parameter changed	Relative photonic efficiency ζ_r		
	3,5-DHT	1,3-DHMB	3,5-DHBA
Reactant concentration[a] (μM)			
100	0.67	0.91	1.29
1000	0.63	1.03	1.33
pH[b]			
3.5	0.83	1.18	1.53
Natural	0.64	1.04	1.13
7.0	1.03	1.01	0.75
9.0	0.99	1.11	0.96
Temperature[c] (K)			
298	0.59	0.96	1.51
303	0.88	0.94	1.45
313	0.88	1.03	1.45
323	0.93	1.18	1.55
333	0.88	1.21	1.38

[a] Conditions: $[TiO_2]$=1 g/l, pH=natural, $I_0=10.8\times10^{-6}$ Einstein/min, T=298 K.
[b] Conditions: $[TiO_2]$=1 g/l, [Reactant]=100 μM, $I_0=10.8\times10^{-6}$ Einstein/min, T=298 K.
[c] Conditions: $[TiO_2]$=1 g/l, [Reactant]=100 μM, pH=natural, $I_0=10.8\times10^{-6}$ Einstein/min.

the ring by attracting electrons towards itself. However, as a result of all the above parameters it is not possible to obtain a general trend according to electronic effects of substituents. Since these substituents are substituted in the *meta* position of the 1,3-DHB ring, they probably do not contribute significantly to the electron density of the ring. Therefore, the concept of relative photonic efficiencies does not have a specific applicability for *meta*-substituted resorcinols.

Quantum yields of the reactants are found from $\phi=\zeta_r\,\phi_{1,3\text{-DHB}}$ at their natural pH as 0.22, 0.35, and 0.38 for 3,5-DHT, 1,3-DHMB and 3,5-DHBA, respectively.

4. Conclusion

A detailed analysis about the incident photon flux and rate of formation of CO_2 for the photocatalytic oxidation of 1,3-DHB is done. It is observed that increasing the number of lamps increases the evolution of CO_2 due to higher production rate of electron–hole pairs. In the mean time, the opportunity of electron–hole recombination also increases. This results in a lower degradation rate.

An integrated sphere model is used to determine the fraction of light absorbed. Increasing the incident photon flux increases the fraction of light absorption. However, the rate of CO_2 formation and degradation of 1,3-DHB decreases. This is due to the increased opportunity of electron–hole recombination. An analogous trend is observed during the calculation of quantum yields with respect to incident photon flux. When the effect of TiO_2 loading is examined for the fraction of light absorption, there is a linear increase up to 1 g/l loading of TiO_2, and then a negative deviation is observed for concentrations higher than 1 g/l of TiO_2. This is because as loading increases the suspension becomes more opaque for the penetration of the light. As a result, rates and quantum yields decrease as a function of TiO_2 loading.

Relative photonic efficiencies of 3,5-DHT, 1,3-DHMB and 3,5-DHB are based on the formation rate of CO_2 in 1,3-DHB. The effect of reactant concentration, pH of the medium and temperature of the system are investigated for the relative efficiencies. No direct relation is found between the electronic efficiencies of the substituents and the relative photonic efficiency. Quantum yields are obtained at the natural pH of reactant molecules.

Acknowledgements

This research was supported by the AVICENNE Research Programme of the European Community (Project No. 074).

References

[1] D.F. Ollis, H. Al-Ekabi, Photocatalytic Purification and Treatment of Water and Air, Elsevier, Amsterdam, 1993, pp. 225–250.
[2] M.A. Fox, T. Dulay, Chem. Rev. 93 (1993) 341.
[3] O. Legrini, E. Oliveros, A.M. Braun, Chem. Rev. 93 (1993) 671.
[4] M.R. Hoffman, S.T. Martin, W. Choi, D.W. Bahnemann, Chem. Rev. 95 (1995) 69.
[5] A. Mills, S. Le Hunte, J. Photochem. Photobiol. A: Chem. 108 (1997) 1.
[6] L. Sun, J.R. Bolton, J. Phys. Chem. 100 (1996) 4127.
[7] I. Rosenberg, J.R. Brock, A. Heller, J. Phys. Chem. 96 (1992) 3423.
[8] N. Serpone, J. Adv. Oxid. Technol. 2 (1997) 203.
[9] N. Serpone, G. Sauve, R. Koch, H. Tahiri, P. Pichat, P. Piccini, E. Pelizetti, H. Hidika, J. Photochem. Photobiol. A: Chem. 94 (1996) 191.
[10] Y. Inel, A.N. Ökte, J. Photochem. Photobiol. A: Chem. 96 (1996) 175.